

Biomechanical stability of internal bone-level implant: Dependency on hex or non-hex structure

Hyeonjong Lee¹, Si-Myung Park², Kwantae Noh³, Su-Jin Ahn⁴, Sangkyun Shin⁵ and Gunwoo Noh*⁵

¹Department of Prosthodontics, School of Dentistry, P.U.S.A.n National University, 49, BU.S.A.ndaehak-ro, Mulgeum-eup, Yangsan-si, Gyeongsangnam-do, 50612, Republic of Korea

²Center for Medical Robotics, Korea Institute of Science and Technology, 5, Hwarang-ro 14-gil, Seongbuk-gu, Seoul, 02792, Republic of Korea

³Department of Prosthodontics, School of Dentistry, Kyung Hee University, 26, Kyungheedae-ro, Dongdaemun-gu, Seoul, 02447, Republic of Korea

⁴Department of Biomaterials & Prosthodontics, Kyung Hee University Hospital at Gangdong, School of Dentistry, Kyung Hee University, 892, Dongnam-ro, Gangdong-gu, Seoul, 05278, Republic of Korea

⁵School of Mechanical Engineering, Kyungpook National University, 80, Daehak-ro, Buk-gu, Daegu, 41566, Republic of Korea

(Received April 29, 2019, Revised December 9, 2017, Accepted November 27, 2019)

Abstract. Considerable controversy surrounds the choice of the best abutment type for implant prosthetics. The two most common structures are hex and non-hex abutments. The non-hex abutment typically furnishes a larger contact area between itself and the implant than that provided by a hex structure. However, when a hex abutment is loaded, the position of its contact area may be deeper than that of a non-hex abutment. Hence, the purpose of this study is to determine the different biomechanical behaviors of an internal bone-level implant based on the abutment type—hex or non-hex—and clinical crown length under static and cyclic loadings using finite element analysis (FEA). The hex structure was found to increase the implant and abutment stability more than the non-hex structure among several criteria. The use of the hex structure resulted in a smaller volume of bone tissues being at risk of hypertrophy and fatigue failure. It also reduced micromovement (separation) between the implant components, which is significantly related to the pumping effect and possible inflammation. Both static and fatigue analyses, used to examine short- and long-term stability, demonstrated the advantages of the hex abutment over the non-hex type for the stability of the implant components. Moreover, although its impact was not as significant as that of the abutment type, a large crown-implant ratio (CIR) increased bone strain and stress in the implant components, particularly under oblique loading.

Keywords: finite element analysis; dental implant; abutment type; fatigue; micromovement

1. Introduction

Implant treatment has become one of the first options for the prosthetic rehabilitation of edentulous and partially-edentulous jaws. An implant abutment system uses a combination of an implant, an abutment having a plurality of connection features for connecting to the implant and an abutment screw for locking the abutment into the implant (Fig. 1). There are several types of abutments for the implants with either a hex or non-hex structure at the connection (Fig. 2). Hex abutments provide rotational position information and anti-rotational effects; however, non-hex abutments are also used in various clinical situations (Lee *et al.* 2017). Although a non-hex abutment provides a greater contact area with the implant than a hex abutment, the position of the contact area of the latter may be deeper than that of the former when it is loaded. Accordingly, the biomechanical advantage of one system over the other remains a subject of debate.

In implant prosthetics, how external forces are

transferred from the occlusal surface to the implant components and surrounding bone should be carefully considered. Several studies on the mechanical stability of implant prosthetics through mechanical loading using a universal testing machine have been conducted (Steinebrunner *et al.* 2008, Apicella *et al.* 2011, Du *et al.* 2015, Westover *et al.* 2016, Romanyk *et al.* 2017). Moreover, finite element analysis (FEA) has been performed to obtain more detailed and visualized results for

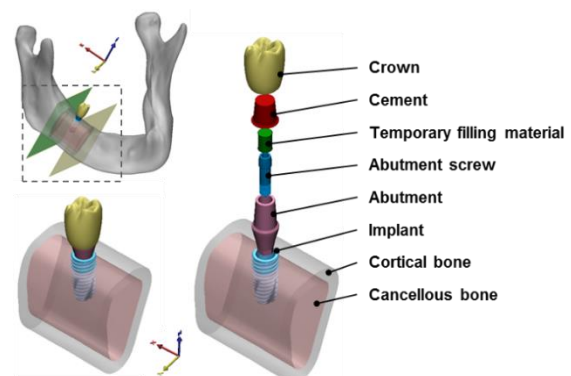


Fig. 1 Structure of the implant complex implanted in the second molar region

*Corresponding author, Assistant Professor
E-mail: gunwoo@knu.ac.kr

each component of the implant complex to better understand the stress distribution in implant prosthetics (Bulaqi *et al.* 2015, Cho *et al.* 2016, Toniollo *et al.* 2016, Farhan *et al.* 2017, Toniollo *et al.* 2017, Amaral *et al.* 2018, Lee *et al.* 2018, Park *et al.* 2018, Pisani *et al.* 2018, Radaelli *et al.* 2018, Lee *et al.* 2019). Recently, FEA was used to evaluate certain biomechanical effects on the bone tissues around the implant caused by various external forces (Verri *et al.* 2014) and the influence of the crown-implant ratio (CIR) on stress distribution (de Moraes *et al.* 2013).

In most FEA implant studies, only static loading applied to the crown was considered (Bergkvist *et al.* 2008, Cho *et al.* 2016, Toniollo *et al.* 2016). Although the results of such loading may provide insights into the stability of the system based on the stress distributions in its components, a fatigue analysis under a cyclic loading condition could provide more meaningful outcomes because it reflects a real-world clinical scenario. For the structural analysis of implants, it is also essential to consider the effect of the preload caused by screw tightening. However, no study has considered such loadings in hex- or non-hex-type abutments. Moreover, although the micro-movements of the implant component are strongly associated with the pumping effect and possible inflammation (Koutouzis *et al.* 2014), these have not been analyzed in terms of the biomechanical stability of the implant complex.

The purpose of this study is to evaluate the stability of implant complexes with two different types of abutment—hex and non-hex—and two different crown lengths based on the mechanical behaviors from the FEA results under static and cyclic loadings. The micro-movements between the contact surfaces were evaluated. The bone strain and the fatigue life of the components in the implant complex were also considered.

2. Finite element models

2.1 Three-dimensional models

A three-dimensional (3D) section of a human right mandible bone around the second molar region was used in this study. The bone segments were derived from computed tomography (CT) data. Segments were demarcated into the cortical (900–1800 Hounsfield Unit; HU) and cancellous bone (150–900 HU) (Papakostas *et al.* 2008) using Mimics v19.0 software (Materialise Group).

A frequently-used implant was chosen as the commercial implant model (TSIII, Osstem) and two types of prosthetic abutments produced by the same company were used. The length of the implant was 10 mm and the diameter was 4 mm. To investigate the effect of the crown height and abutment base shape on the stability of the implant complex, four 3D models were constructed (Fig. 2). The 3D models were modeled to have different CIRs (1.0 and 1.5) by scaling the upper part of the abutment—above the plane parallel to the bottom of the crown—as crown height increased. Two models had hex and two had non-hex connection abutments. The surface contact area differed based on the abutment type, as illustrated in Fig. 3.

An abutment screw (EbonyGold, Osstem) was used to fix the implant to the abutment and a cement layer and temporary filling material were used as adhesive material between the crown and abutment. The complete model consisted of the crown, cement layer, temporary filling material, abutment screw, abutment, implant, cancellous bone and cortical bone (Fig. 1), which were assembled in 3-matic 3D modeling software (Materialise Group) and exported to Abaqus v6.14 software (Dassault Systèmes SIMULIA Corp.).

2.2 Material properties and mesh

The components of the implant system and the surrounding bone were assumed to be isotropic, homogenous and linearly elastic. Material properties are presented in Table 1 (Barbier *et al.* 1998, Niinomi 1998, Wierszycki *et al.* 2006, Tolidis *et al.* 2012, Rungsiyakull *et al.* 2015). Titanium alloy (6AL-4V-ELI) (Niinomi 1998, Wierszycki *et al.* 2006) was used for the implant, abutment and abutment screw and ceramic (Rungsiyakull *et al.* 2015) was used for the crown in the FEAs.

Each component was divided into four-node tetrahedral elements and the element size was densely set for the contact surfaces, screw, implant and bone. The number of nodes and elements of each model are listed in Table 2. Table 3 shows the results of the convergence test to determine the element sizes (Szwedowski *et al.* 2011).

2.3 Interactions

Contact is defined using surface-to-surface discretization because it provides more accurate stress and pressure results than node-to-surface discretization (Djebbar *et al.* 2015). As illustrated in Fig. 3, “Contact 1” refers to the contact area between the abutment and screw and “Contact 2” refers to the contact area between the abutment and implant. The friction coefficient of the surface abutting the conical seal of the screw is 0.441 and that of the implant surface abutting the base surface is 0.16 (Guda *et al.* 2008, Wang *et al.* 2009). In each model, the abutment and implant were firmly engaged with each other by tightening the screw and the surface contact area differed based on the abutment type (Fig. 3). The other interactions incorporating bonding materials, cement and bone were simulated as tie conditions because we assumed perfect osseointegration.

3. Boundary condition and loading condition

The boundary conditions were established as fixed in all axes (x, y and z) at the distal and mesial planes in the block section (Fig. 4). All finite element models were built and analyzed using Abaqus 6.14 software (Dassault Systèmes SIMULIA Corp.).

3.1 Preload

When the abutment screw is tightened, a tightening torque is applied as a moment to the head of the abutment screw, which induces a contact force in the interface

Table 1 Material properties used in the finite element model

	6AL-4V-ELI*	Ceramic crown	Cement	Cortical bone	Cancellous bone	Temporary filling material
Young's modulus (MPa)	110 000	140 000	10 760	13 700	1 370	15 000
Poisson ratio	0.34	0.28	0.35	0.3	0.3	0.3
Yield stress /UTS**(MPa)	860/ 1004	-	-	-	-	-
Reference	Niinomi 1998, Wierszycki <i>et al.</i> 2006	Rungsiyakull <i>et al.</i> 2015	Tolidis <i>et al.</i> 2012	Barbier <i>et al.</i> 1998	Barbier <i>et al.</i> 1998	Rungsiyakull <i>et al.</i> 2015

* Titanium material: abutment, abutment screw, implant

** Ultimate tensile stress

Table 2 Number of tetrahedral elements in each model

Connection type	Hex		Non-hex	
CIR*	1.0	1.5	1.0	1.5
Elements	1 766 964	1 885 361	1 770 291	1 887 073
Nodes	319 016	346 257	319 347	346 382

* Crown-Implant Ratio

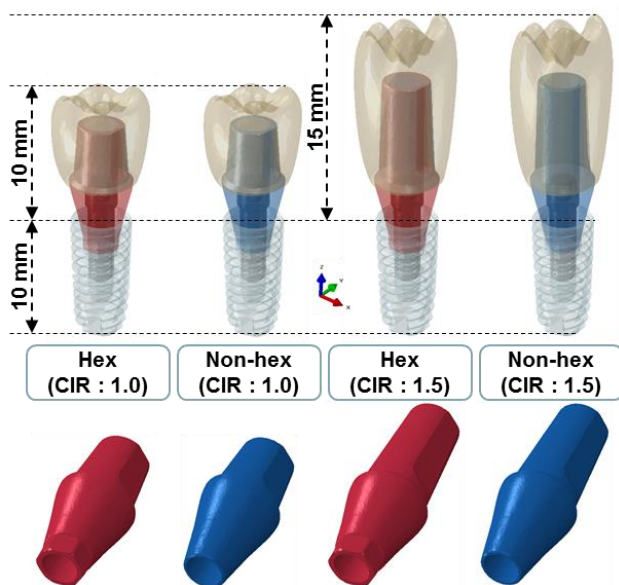


Fig. 2 Dimensions of the four finite element models consisting of different abutment connection types (hex or non-hex) and different CIRs (1.0 or 1.5)

between the abutment and implant that are clamped together. This contact force clamping together the abutment and the implant is called the preload (Patterson and Johns 1992). The accuracy of the preload reached during screw tightening and clamping of the abutment and implant together becomes essential for studying the behavior of the implant complex. In this study, the amount of preload—achieved by a torque of 32 N·cm applied to the screw during tightening—was calculated using the formula described in previous studies (Lang *et al.* 2003, Lopez-Arancibia *et al.* 2015, Wang *et al.* 2018). During the calculation of the preload in this study, the geometrical relationship between the abutment and implant fixed by the screws was considered.

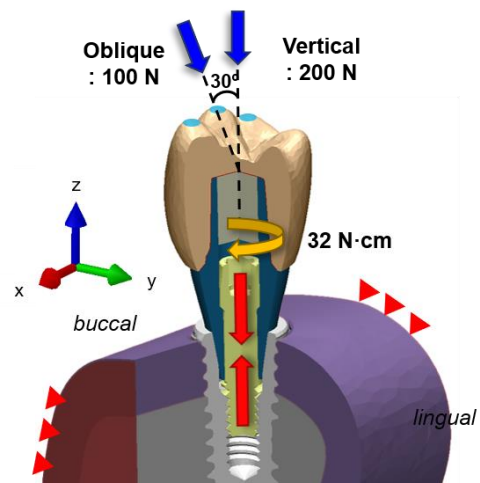


Fig. 4 Loading conditions applied to each finite element model. The red arrows indicate the preload resulting from a torque of 32 N·cm (yellow arrow). The blue arrows indicate the two types of biting forces applied. Both ends of the bone fragment were fixed in all directions.

3.2 External biting load

To evaluate the stability of the implant complex, two loading conditions—commonly known as the biting forces on the second molar region (Junior *et al.* 2013)—were considered: (1) a force of 200 N applied to 30 nodes on 3 cusps in the vertical direction and (2) a force of 100 N to 30 nodes on 3 cusps in the oblique direction. The oblique force was set at a 30-degree angle relative to the long axis of the implant from the buccal to the lingual direction (Fig. 4).

3.3 Fatigue analysis

To predict the number of repetitions required until failure of the implant components comprised of Ti-6AL-4V ELI (Table 1), a computational fatigue analysis was

Table 3 Mean of the maximum stress results in each component

Load type	Oblique loading				Vertical loading			
	1.0*	1.5	1.75	2.0	1.0*	1.5	1.75	2.0
Relative element size	1.0*	1.5	1.75	2.0	1.0*	1.5	1.75	2.0
hex abutment	41.871	38.444	38.471	37.215	44.009	40.083	40.633	37.215
abutment screw	104.672	100.777	103.449	104.157	106.909	107.006	108.829	104.157
crown	6.343	6.713	7.214	5.858	10.509	11.071	11.782	5.858
cement	4.613	4.205	4.281	5.683	6.467	5.904	5.835	5.683
cortical bone	1.63e-04	1.56e-04	1.54e-04	1.41e-04	2.11e-04	2.05e-04	2.00e-04	1.41e-04
cancellous bone	1.62e-04	1.67e-04	1.70e-04	1.64e-04	3.19e-04	3.34e-04	3.31e-04	1.64e-04
temporary filling material	1.393	1.406	1.490	1.865	1.325	1.317	1.393	1.865
implant	19.693	18.066	19.592	19.446	23.989	20.589	21.821	19.446

* The relative characteristic element size of 1.0 was used in the following finite element analysis

performed in the FE-Safe/Composites™ program. This program uses advanced multiaxial fatigue algorithms containing a multiaxial plasticity model (Wierszycki *et al.* 2006, El Sallah *et al.* 2016, Mohamed *et al.* 2016, Mohamed *et al.* 2018). These algorithms are based on the stress results obtained from the FEA (Fig. 7), variations in loading, hysteresis loop cycle closure and cyclic material properties. Repetitive mastication in the analysis was assumed to be the alternating application of an oblique load of 100 N and a vertical load of 200 N, whereas the biting force applied to the second molar was assumed to be approximately 50 N (Santiago *et al.* 2013). Elastic stresses from the FEA model were converted to elastic-plastic stresses by using a biaxial Neuber's rule and cyclic material properties (Topper *et al.* 1967). A rainflow cycle-counting algorithm was used to extract fatigue cycles (Amzallag *et al.* 1994). For biaxial fatigue methods, a critical plane procedure was used to calculate the orientation of the most-damaged plane at the node. Finally, the program calculated the factor of strength (FOS) by which the stresses at each node can be increased or reduced to produce the required life (ABAQUS/Safe Manual, Bishop and Sherratt 2000, Draper 1999).

4. Result

4.1 Principal strain distributions on the bone

Minimum principal strain distributions on the bone segments are illustrated in Figs. 5(a)-(b). In the cortical and cancellous bone, maximum strain values were found primarily in the peri-implant bone tissue at the apical part of the implant and its interface with the cortical bone. The results obtained with the application of vertical force exhibited similar strain distribution patterns regardless of the abutment type and CIR. The strain was predominantly concentrated on the buccal side, where the vertical force was applied. However, under oblique loading, maximum strain values were observed primarily at the opposite side of the load application and a larger area with a strain of over 2500 $\mu\epsilon$ was observed with a CIR of 1.5 than that obtained with a CIR of 1.0.

Fig. 5(b) illustrates the volume of the bone elements near the implant where bone remodeling is likely to occur, classified based on the strain value level (Roberts *et al.* 2004). The volume of bone tissues that could cause bone hypertrophy was less than 1 mm³, whereas the volume exhibiting a risk of fracture was less than 0.2 mm³ even though the hex connection exhibited more stability than the non-hex connection.

4.2 Implant components

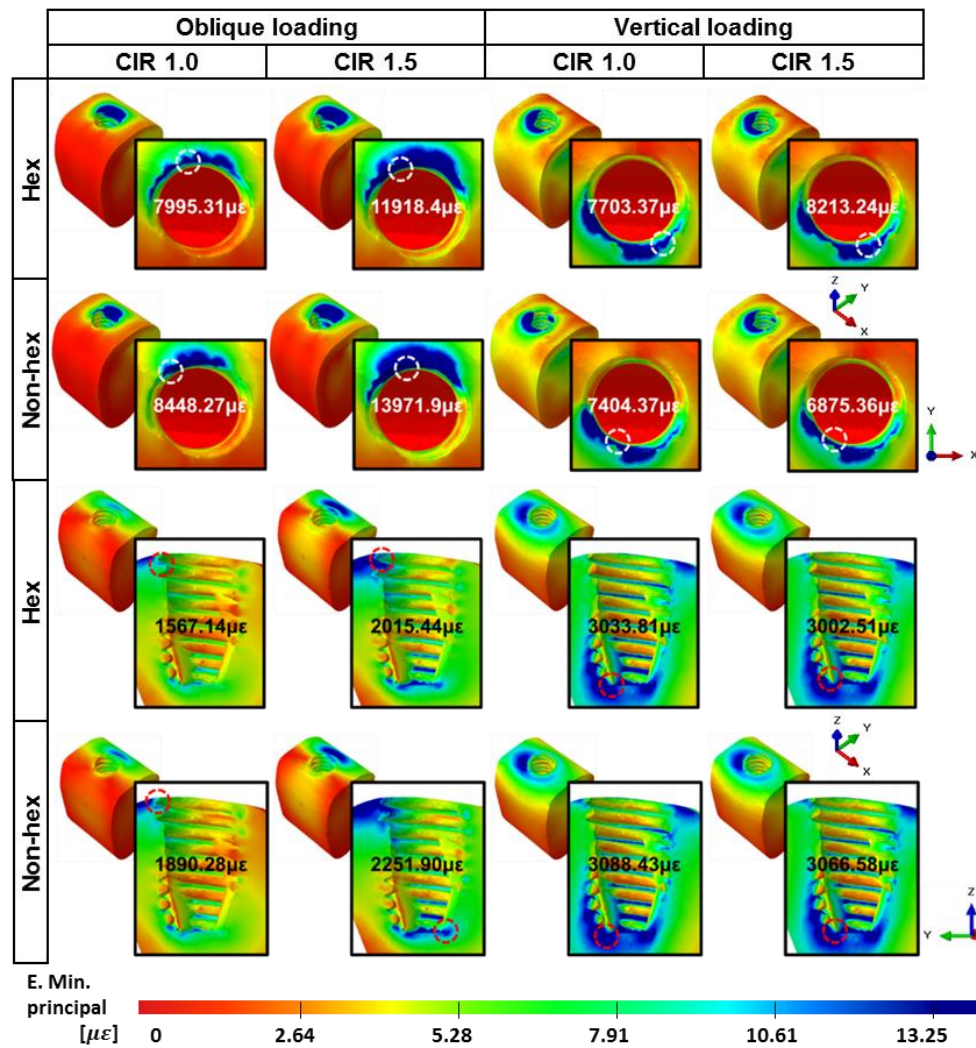
4.2.1 Separations between contact areas

The distribution of the separations between the components of the implant complex is illustrated in Fig. 6. The colors closer to blue represent the occurrence of larger separations. By scrutinizing the separation distributions in Contact 1, the movement of the abutment caused by the external load may be analyzed. When the oblique load was applied, the abutment moved down in the lingual direction and was separated from the conical seal of the abutment screw. In contrast, when the vertical load was applied, a downward movement of the abutment in the buccal direction was observed. Moreover, movements of the abutment were more prominent when a non-hex connection was used: the separations at Contact 2 were approximately twice those of the hex connection. However, there was no consistent trend regarding separations at different CIR values.

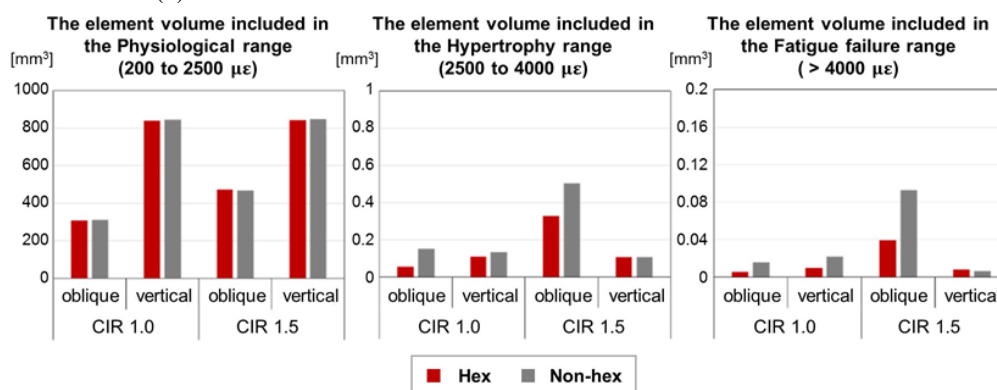
4.2.2 von Mises stress distribution

To examine stresses among implant components more closely, stress values at contact surfaces were observed (Fig. 7). With a CIR of 1.5 and applied oblique load, the maximum stress of the non-hex connection at both contact surfaces was beyond the titanium alloy yield point of 860 MPa. However, for the hex connection, the maximum values of the stress at all contact surfaces remained within the elastic range. Different abutment connection types caused more pronounced changes in stress distribution in the implant than different CIRs. The maximum stress values of the non-hex connection were higher than those of the hex connection in all cases.

Under applied oblique load and with a larger CIR,



(a) Strain distributions within the cortical bone and cancellous bone



(b) The graph of the element volume divided by strain range

Fig. 5 The result of the strain

higher stresses were observed on both contact surfaces. However, under applied vertical load, an increase in crown height did not deteriorate stress distribution in the abutment-implant interface.

4.2.3 Fatigue analysis

The estimated repetitions required for the fatigue failure of components made of titanium alloys and the locations

where fractures occur are illustrated in Fig. 8. These repetitions pertain to the cycles of vertical loading followed by oblique loading. Moreover, the resulting fatigue endurance of both abutment types was better for a CIR of 1.0 than for a CIR of 1.5 and the implant complex with a hex connection had higher fatigue endurance for both the abutment and implant. This study predicted that fatigue failure will not occur within 1×10^7 repetitions in abutments

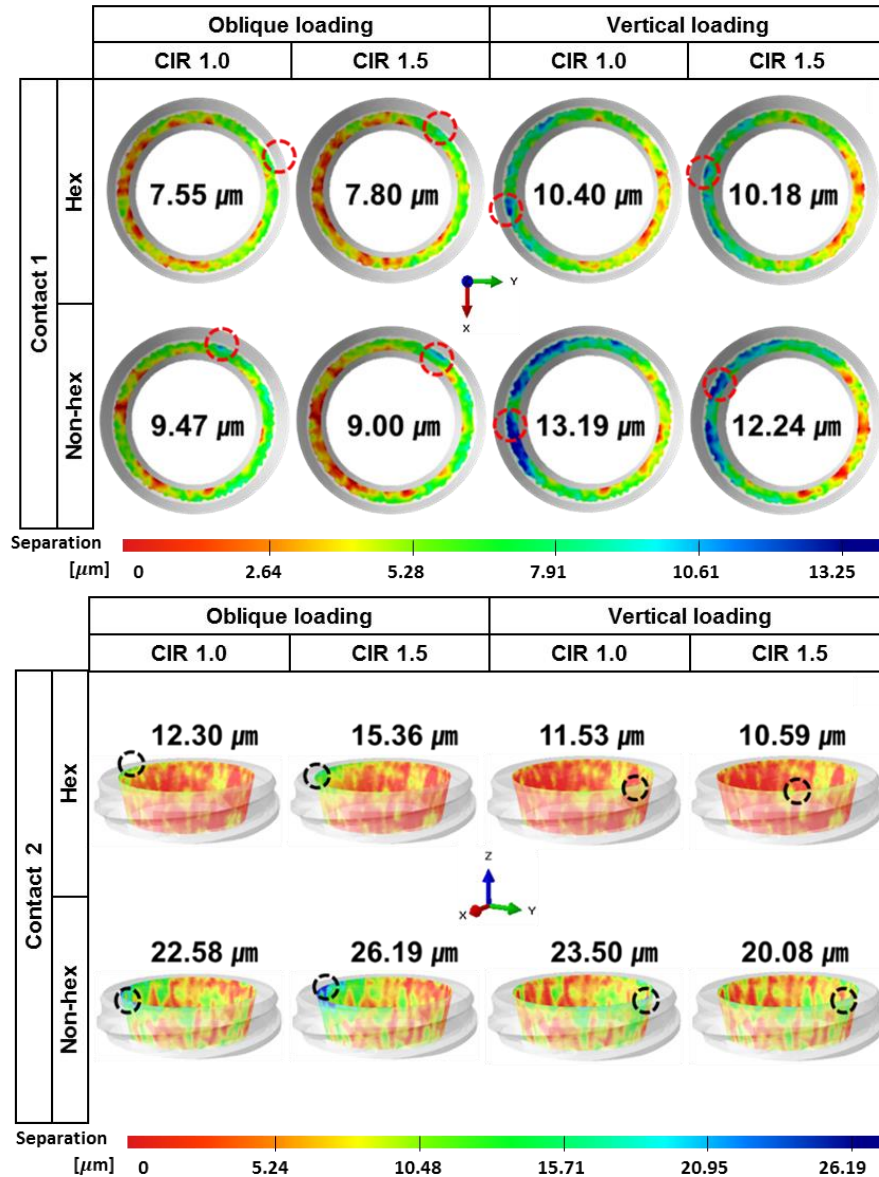


Fig. 6 Micro-movements (separations) between implant components within Contacts 1 and 2.

with hex connections. The hex connection implants with CIRs of 1.0 and 1.5 had 45.8 and 5.97 times longer lives than those of the non-hex connection implants.

5. Discussion

Although hex and non-hex abutments continue to be widely used in implant prosthetics, there is much controversy about which abutment type can deliver superior biomechanical stability. Previous studies have been limited to examining the impact of different contact surfaces, which is a conspicuous feature depending on the abutment type. Therefore, a lack of knowledge of the mechanism by which load is transferred from the crown surface to the implant components and of the resulting biomechanical stability, remains. Accordingly, in this study, the differences between hex and non-hex abutments were analyzed with a greater

focus on the relationship of contact surfaces. Furthermore, by considering preload, an external biting load and repetitive external load, all implant components were analyzed for both short- and long-term stability under adequate intrinsic prestress.

As illustrated in Fig. 3, the two abutment types have different tightly-engaged contact areas. The area of the tightly-engaged surface of the hex abutment was approximately 67% that of the non-hex abutment, which is typical in most bone-level implants. External forces are often considered to be primarily transferred through a tightly engaging surface and it is also accepted that the stress value may be reduced by increasing its contact area. Hence, the stress is expected to be lower in the non-hex abutment compared with the hex abutment. However, because the hex structure significantly improves stress distribution, the hex connection had approximately 65% to 75% of the stress values of the non-hex connection, both in

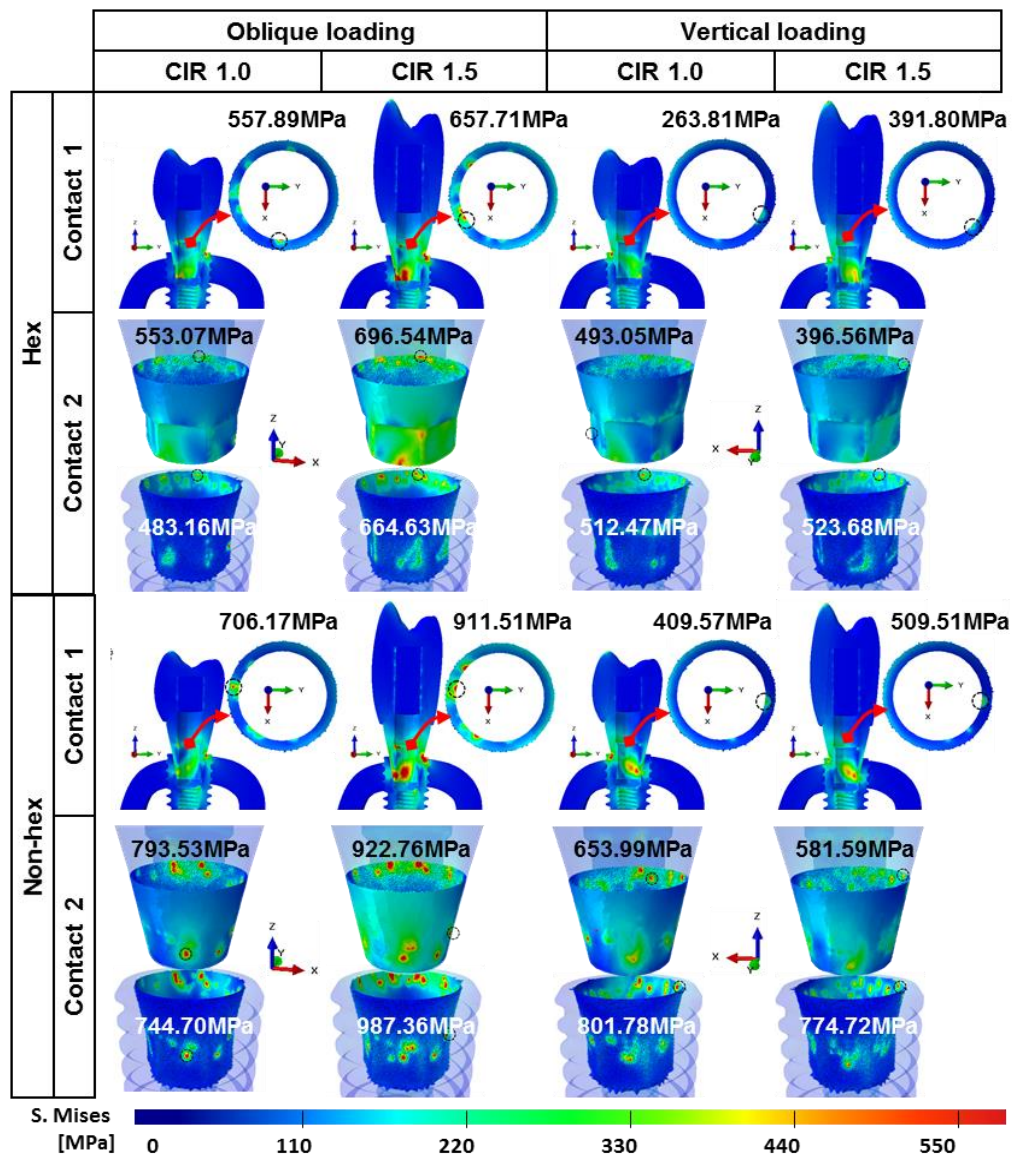


Fig. 7 Stress distribution on the contact surfaces in Contacts 1 and 2. The black dashed circles indicate the location of the maximum stress value on the surface

the abutment and implant (Fig. 7). Furthermore, it was expected that the micro-movements between the implant components would be prevented during the loading phase (Fig. 4) as the clamping force after the screw-tightening process was applied for the tightly-engaged contact surfaces. The micro-movement between the implant components is important because of its association with the pumping effect and inflammation (Koutouzis *et al.* 2014). However, the micro-movements of the two engaged contact surfaces were observed in each group, confirming the definitive advantage of the hex group over the non-hex group in reducing micro-movement (Fig. 6). Furthermore, it was verified that the difference in CIR rarely affects micro-movement.

These unexpected results indicate that potential contact surfaces (Fig. 3), which were assumed to have less impact than tightly-engaged contact surfaces, have an important influence on the behavior of implant components. Kim and Cho (2016) described incomplete contact due to the

approximately 10 μm gap between the hex abutment and implant surface. However, when the load was applied, the hex structure made contact with the internal surface of the implant and distributed the stress from the abutment to the implant (Fig. 7). The result of this additional stress distribution was more prominent in the fatigue analysis (Fig. 8). Therefore, the implant contact behavior is affected not only by the tightly-engaged contact area but also by the potential contact area. In contrast, the impact of a large CIR was not as significant as that of the abutment type, despite the external loading being applied directly to the crown. Thus, the internal contact area has a greater effect than external loading area.

Strain values of the bone surrounding the transplanted implant are significant risk indicators. According to Roberts *et al.* (2004), a strain value of more than 2500 $\mu\epsilon$ indicates the risk of hypertrophy because bone formation occurs more rapidly than resorption in the bone modeling process.

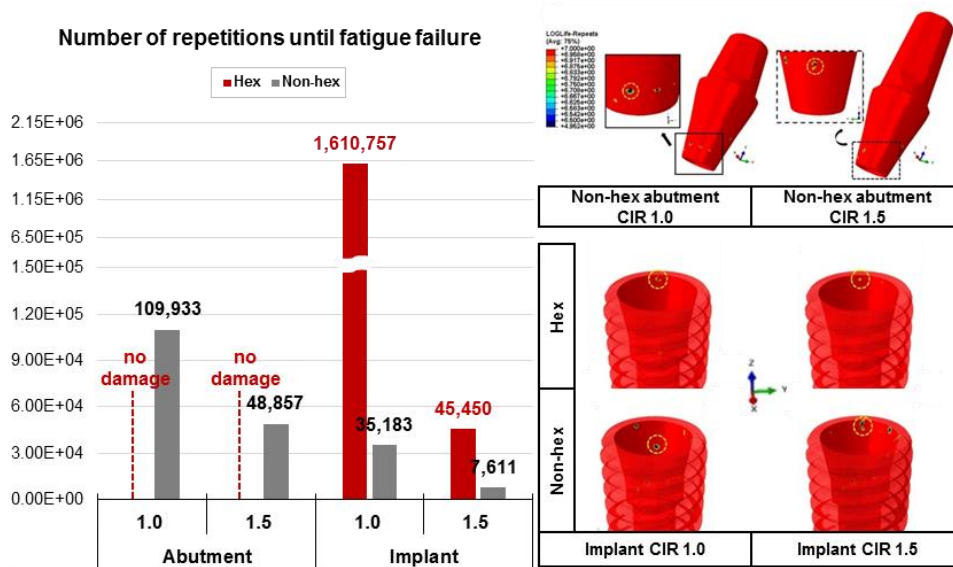


Fig. 8 Fatigue analysis. Yellow dashed circles indicate the locations most vulnerable to fatigue failure.

A strain value of more than $4000 \mu\epsilon$ can lead to fatigue failure of the bone. The peak strain in each group is illustrated in Fig. 5(a) and the element volumes corresponding to three different categories are illustrated in Fig. 5(b). The non-hex with 1.5 CIR group yielded a higher element volume in the hypertrophy and fatigue failure range and the rate of bone formation was less than that of bone resorption in the fatigue failure range. However, the risk of a catastrophic fracture is negligible if the micro-strain is below $2500 \mu\epsilon$ and the masticatory force is not applied continuously (Roberts et al. 2004). In all groups, the bone around the implant can physiologically sustain the strain.

6. Conclusions

In this study, two implant complexes with different abutment structures were analyzed for short- and long-term stability. The stress in the hex group was 73% that of the non-hex group. Although the non-hex abutment had a wider tightly-engaged contact surface, micro-movement was lower and more uniform when hex abutment was used. The relatively uniform micro-movements induced a lower stress concentration at the contact between the abutment and implant, which provided longer life for implant components and long-term stability. The impact on the stability of the implant complex is greater in the relationship between internal contact surfaces than in the relationship between the crown and implant. While the required values employed to perform FEA were based on existing studies to closely approximate real-world clinical situations, this study had several limitations. First, the material properties of components were assumed to be isotropic and linearly elastic. Second, we assumed a complete bond between the implant and the surrounding bone. For more reliable solutions, experimental validations of FE models would be valuable.

Acknowledgments

The research was supported by the Basic Science Research Program (Grant No. 2018R1D1A1B07049789) through the National Research Foundation of Korea (NRF) funded by the Ministry of Education.

References

- ABAQUS/Safe User's Manual (2001), HKS, Inc. Pawtucket.
- Amaral, C.F., Gomes, R.S., Garcia, R.C.R. and Cury, A.A. D.B. (2018), "Stress distribution of single-implant-retained overdenture reinforced with a framework: A finite element analysis study", *J. Prosthet. Dent.*, **119**(5), 791-796. <https://doi.org/10.1016/j.prosdent.2017.07.016>.
- Amzallag, C., Gerey, J. P., Robert, J. L. and Bahaud, J. (1994), "Standardization of the rainflow counting method for fatigue analysis", *Int. J. Fatigue*, **16**(4), 287-293. [https://doi.org/10.1016/0142-1123\(94\)90343-3](https://doi.org/10.1016/0142-1123(94)90343-3).
- Apicella, D., Veltri, M., Balleri, P., Apicella, A. and Ferrari, M. (2011), "Influence of abutment material on the fracture strength and failure modes of abutment-fixture assemblies when loaded in a bio-faithful simulation", *Clin. Oral Implants Res.*, **22**(2), 182-188. <https://doi.org/10.1111/j.1600-0501.2010.01979.x>.
- Barbier, L., Sloten, J. V., Krzesinski, G. and Van Der Perre, E. S. G. (1998), "Finite element analysis of non-axial versus axial loading of oral implants in the mandible of the dog", *J. Oral Rehabil.*, **25**(11), 847-858. <https://doi.org/10.1046/j.1365-2842.1998.00318.x>.
- Bergkvist, G., Simonsson, K., Rydberg, K., Johansson, F. and Dérand, T. (2008), "A finite element analysis of stress distribution in bone tissue surrounding uncoupled or splinted dental implants", *Clin. Implant Dent. Relat. Res.*, **10**(1), 40-46. <https://doi.org/10.1111/j.1708-8208.2007.00059.x>.
- Bishop, N. W. and Sherratt, F. (2000), "Finite element based fatigue calculations", *NAFEMS*.
- Bulaqi, H.A., Mashhadi, M.M., Safari, H., Samandari, M.M. and Gerampanah, F. (2015), "Effect of increased crown height on stress distribution in short dental implant components and their surrounding bone: A finite element analysis", *J. Prosthet. Dent.*,

- 113(6), 548-557. <https://doi.org/10.1016/j.prosdent.2014.11.007>.
- Cho, S. Y., Huh, Y. H., Park, C. J. and Cho, L. R. (2016), "Three-Dimensional Finite Element Analysis of the Stress Distribution at the Internal Implant-Abutment Connection", *Int. J. Periodontics Restorative Dent.*, **36**(3). <http://doi.org/10.11607/prd.2351>.
- Du, J., Lee, J.H., Jang, A.T., Gu, A., Hossaini-Zadeh, M., Prevost, R., Curtis, D.A. and Ho, S.P. (2015), "Biomechanics and strain mapping in bone as related to immediately-loaded dental implants", *J. Biomech.*, **48**(12), 3486-3494. <https://doi.org/10.1016/j.jbiomech.2015.05.014>.
- Djebbar, N., Serier, B. and Bouiadjra, B.B. (2015), "Finite element analysis in static and dynamic behaviors of dental prosthesis", *Struct. Eng. Mech.*, **55**(1), 65-78. <http://dx.doi.org/10.12989/sem.2015.55.1.065>.
- Draper, J. (1999). "Modern metal fatigue analysis". *HKS. Inc. Pawtucket*.
- El Sallah, Z.M., Smail, B., Abderahmane, S., Bouiadjra, B.B. and Boualem, S. (2016), "Numerical simulation of the femur fracture under static loading", *Struct. Eng. Mech.*, **60**(3), 405-412. <http://dx.doi.org/10.12989/sem.2016.60.3.405>.
- Farhan, A.M. (2017), "Effect of magnetic field on wave propagation in cylindrical poroelastic bone with cavity", *Struct. Eng. Mech.*, **61**(4), 539-549. <http://dx.doi.org/10.12989/sem.2017.61.4.539>.
- Guda, T., Ross, T.A., Lang, L.A. and Millwater, H.R. (2008), "Probabilistic analysis of preload in the abutment screw of a dental implant complex", *J. Prosthet. Dent.*, **100**(3), 183-193. [https://doi.org/10.1016/S0022-3913\(08\)60177-8](https://doi.org/10.1016/S0022-3913(08)60177-8).
- Junior, J.F.S., Pellizzer, E.P., Verri, F.R. and de Carvalho, P. S. P. (2013), "Stress analysis in bone tissue around single implants with different diameters and veneering materials: a 3-D finite element study", *Mater. Sci. Eng. C*, **33**(8), 4700-4714. <https://doi.org/10.1016/j.msec.2013.07.027>.
- Kim, Y.H. and Cho, H.W. (2016), "Comparison of marginal and internal fit of zirconia abutments with titanium abutments in internal hexagonal implants", *J. Korean Acad. Prosthodont.*, **54**(2), 93-102. <http://doi.org/10.4047/jkap.2016.54.2.93>.
- Koutouzis, T., Mesia, R., Calderon, N., Wong, F. and Wallet, S. (2014), "The effect of dynamic loading on bacterial colonization of the dental implant fixture-abutment interface: an in vitro study", *J. Oral Implantol.*, **40**(4), 432-437. <https://doi.org/10.1563/AAID-JOI-D-11-00207>.
- Lang, L.A., Kang, B., Wang, R.F. and Lang, B.R. (2003), "Finite element analysis to determine implant preload", *J. Prosthet. Dent.*, **90**(6), 539-546. <https://doi.org/10.1016/j.prosdent.2003.09.012>.
- Lee, H., Kwon, K.R., Paek, J., Pae, A. and Noh, K. (2017), "A Method for Minimizing Rotational Errors of Implant Prostheses", *Int. J. Oral Maxillofac. Implants*, **32**(5). <http://doi.org/10.11607/jomi.5324>.
- Lee, H., Park, S. and Noh, G. (2019), "Biomechanical analysis of 4 types of short dental implant in a resorbed mandible", *J. Prosthet. Dent.*, **121**(4), 659-670. <https://doi.org/10.1016/j.prosdent.2018.07.013>.
- Lee, J.S., Choi, H.I., Lee, H., Ahn, S.J. and Noh, G. (2018), "Biomechanical effect of mandibular advancement device with different protrusion positions for treatment of obstructive sleep apnoea on tooth and facial bone: A finite element study", *J. Oral Rehabil.*, **45**(12), 948-958. <https://doi.org/10.1111/joor.12709>.
- Lopez-Arancibia, A., Altuna-Zugasti, A. M., Aldasoro, H. A. and Pradera-Mallabiarrena, A. (2015), "Bolted joints for single-layer structures: numerical analysis of the bending behavior", *Struct. Eng. Mech.*, **56**(3), 355-367. <https://doi.org/10.12989/sem.2015.56.3.355>.
- Mohamed, C., Smail, B., Bouiadjra, B. and Serier, B. (2016), "Numerical model of the damage, around inclusion in the orthopedic cement PMMA", *Struct. Eng. Mech.*, **57**(4), 717-731. <https://doi.org/10.12989/sem.2016.57.4.717>.
- Mohamed, C., Abderahmane, S. and Benbarek, S. (2018), "Fracture behavior modeling of a 3D crack emanated from bony inclusion in the cement PMMA of total hip replacement", *Struct. Eng. Mech.*, **66**(1), 37-43. <https://doi.org/10.12989/sem.2018.66.1.037>.
- Moraes, S.L.D.D., Verri, F.R., Junior, J.F.S., Almeida, D.A. D.F., Mello, C.C.D. and Pellizzer, E.P. (2013), "A 3-D finite element study of the influence of crown-implant ratio on stress distribution", *Braz. Dent. J.*, **24**(6), 635-641. <http://dx.doi.org/10.1590/0103-6440201302287>.
- Niinomi, M. (1998), "Mechanical properties of biomedical titanium alloys", *Mater. Sci. Eng. A*, **243**(1-2), 231-236. [https://doi.org/10.1016/S0921-5093\(97\)00806-X](https://doi.org/10.1016/S0921-5093(97)00806-X).
- Papakostas, G.I., McGrath, P., Stewart, J., Charles, D., Chen, Y., Mischoulon, D., Dording, C. and Fava, M. (2008), "Psychic and somatic anxiety symptoms as predictors of response to fluoxetine in major depressive disorder", *Psychiatry Res.*, **161**(1), 116-120. <https://doi.org/10.1016/j.psychres.2008.02.011>.
- Park, S.M., Lee, J.W. and Noh, G. (2018), "Which plate results in better stability after segmental mandibular resection and fibula free flap reconstruction? Biomechanical analysis", *Oral Surg. Oral Med. Oral Pathol. Oral Radiol. Endod.*, **126**(5), 380-389. <https://doi.org/10.1016/j.oooo.2018.05.048>.
- Patterson, E.A. and Johns, R.B. (1992), "Theoretical analysis of the fatigue life of fixture screws in osseointegrated dental implants", *Int. J. Oral. Maxillofac. Implants*, **7**(1), 26-33.
- Pisani, M.X., Presotto, A.G.C., Mesquita, M.F., Barão, V.A.R., Kemmoku, D.T. and Cury, A.A.D.B. (2018), "Biomechanical behavior of 2-implant-and single-implant-retained mandibular overdentures with conventional or mini implants", *J. Prosthet. Dent.*, **120**(3), 421-430. <https://doi.org/10.1016/j.prosdent.2017.12.012>.
- Radaelli, M.T.B., Idogava, H.T., Spazzin, A.O., Noritomi, P.Y. and Boscato, N. (2018), "Parafunctional loading and occlusal device on stress distribution around implants: A 3D finite element analysis", *J. Prosthet. Dent.*, **120**(4), 565-572. <https://doi.org/10.1016/j.prosdent.2017.12.023>.
- Roberts, W.E., Huja, S. and Roberts, J.A. (2004), "Bone modeling: biomechanics, molecular mechanisms and clinical perspectives", *Semin. Orthod.*, **10**(2), 123-161. <https://doi.org/10.1053/j.sodo.2004.01.003>.
- Romanyk, D.L., Guan, R., Major, P.W. and Dennison, C.R. (2017), "Repeatability of strain magnitude and strain rate measurements in the periodontal ligament using fibre Bragg gratings: An ex vivo study in a swine model", *J. biomech.*, **54**, 117-122. <https://doi.org/10.1016/j.jbiomech.2017.01.047>.
- Rungsiyakull, C., Chen, J., Rungsiyakull, P., Li, W., Swain, M. and Li, Q. (2015), "Bone's responses to different designs of implant-supported fixed partial dentures", *Biomech. Model. Mechanobiol.*, **14**(2), 403-411. <https://doi.org/10.1007/s1023>.
- Steinebrunner, L., Wolfart, S., Ludwig, K. and Kern, M. (2008), "Implant-abutment interface design affects fatigue and fracture strength of implants", *Clin. Oral Implants Res.*, **19**(12), 1276-1284. <https://doi.org/10.1111/j.1600-0501.2008.01581.x>.
- Szwedowski, T.D., Fialkov, J. and Whyne, C.M. (2011), "Sensitivity analysis of a validated subject-specific finite element model of the human craniofacial skeleton", *Proc. Institution Mech. Engineers, Part H J. Eng. Medicine*, **225**(1), 58-67. <https://doi.org/10.1243/09544119JEIM786>.
- Tolidis, K., Papadogiannis, D., Papadogiannis, Y. and Gerasimou, P. (2012), "Dynamic and static mechanical analysis of resin luting cements", *J. Mech. Behav. Biomed. Mater.*, **6**, 1-8. <https://doi.org/10.1016/j.jmbbm.2011.10.002>.
- Toniollo, M.B., Macedo, A.P., Pupim, D., Zapparoli, D. and de Mattos, M.D.G.C. (2016), "Three-dimensional finite element analysis surface stress distribution on regular and short Morse taper implants generated by splinted and nonsplinted prostheses in the rehabilitation of various bony ridges", *J. Craniofac. Surg.*, **27**(3),

- e276-e280. <http://doi.org/10.1097/SCS.0000000000002520>.
- Toniollo, M.B., Macedo, A.P., Silveira Rodrigues, R.C., Ribeiro, R.F. and da Gloria Chiarello de Mattos, M. (2017), "A Three-Dimensional Finite Element Analysis of the Stress Distribution Generated by Splinted and Nonsplinted Prostheses in the Rehabilitation of Various Bony Ridges with Regular or Short Morse Taper Implants", *Int. J. Oral Maxillofac. Implants*, **32**(2). <http://doi.org/10.11607/jomi.4696>.
- Topper, T., Wetzel, R. M. and Morrow, J. (1967), "Neuber's rule applied to fatigue of notched specimens", Illinois University at Urban Department of Theoretical and Applied Mechanics, <https://apps.dtic.mil/dtic/tr/fulltext/u2/659550.pdf>.
- Verri, F.R., de Souza Batista, V.E., Santiago Jr, J.F., de Faria Almeida, D.A. and Pellizzer, E.P. (2014), "Effect of crown-to-implant ratio on peri-implant stress: a finite element analysis", *Mater. Sci. Eng. C*, **45**, 234-240. <https://doi.org/10.1016/j.msec.2014.09.005>.
- Wang, R.F., Kang, B., Lang, L.A. and Razzoog, M.E. (2009), "The dynamic natures of implant loading", *J. Prosthet. Dent.*, **101**(6), 359-371. [https://doi.org/10.1016/S0022-3913\(09\)60079-2](https://doi.org/10.1016/S0022-3913(09)60079-2).
- Wang, L. and Su, R.K.L. (2018), "Strengthening of preloaded RC columns by post compressed plates - A review", *Struct. Eng. Mech.*, **65**, 477-490. <http://doi.org/10.12989/sem.2018.65.4.477>.
- Westover, L., Faulkner, G., Hodgetts, W. and Raboud, D. (2016), "Advanced system for implant stability testing (ASIST)", *J. Biomech.*, **49**(15), 3651-3659. <https://doi.org/10.1016/j.jbiomech.2016.09.043>.
- Wierszycki, M., Kąkol, W. and Łodygowski, T. (2006), "The screw loosening and fatigue analyses of three dimensional dental implant model", *In ABAQUS Users' Conference 2006*, Boston, U.S.A., May.